Multispectrum Approach in Quantitative EEG: Accuracy and Physical Effort

Aimé Lay-Ekuakille, *Senior Member, IEEE*, Patrizia Vergallo, Diego Caratelli, Francesco Conversano, Sergio Casciaro, and Antonio Trabacca

***Abstract*— The detection of neurophysiological features by means of electroencephalogram (EEG) is one of the most recurrent medical exams to be performed on human beings. As it stands, EEG trials are not always sufficient to deliver a clear and precise diagnosis for much pathology. Hence, it must be integrated with other exams. However, we can use all additional instrumental exams to improve the quality of the diagnosis because there are other constraints, namely, financial, medical, and individual. This paper presents an original implementation of EEG signal processing using filter diagonalization method to build a bispectrum and contour representation to discover possible abnormalities hidden in the signal for aided-diagnosis. Two different EEG signals are used for this scope. EEG signals are acquired simultaneously with electrocardiograms (ECG) and ergospirometric ones. ECG signals are also processed along with EEGs. A comparison is made with high order spectra approach. All experimental data regarding EEG, ECG, and ergospirometry are acquired during suspected-patient walking along a path of ∼32 m for verifying the impact of fatigue on neurophysiological processes and vice versa.**

***Index Terms*— Neurophysiology, EEG, ECG, ergospirometry, heart rate, multispectrum analysis, epilepsy, accuracy.**

I. Introduction

WORKING with EEG for neurophysiology characterization is mostly used in many hospital and biomedical research centres. The main scope is often detecting impairments and preliminary diagnosis approach. However, EEGs are used for studying epilepsy [1]. The vast majority of EEG acquisition [2], for clinical studies, is made from electrodes glued onto standard locations on the scalp. These electrodes average the action potentials from large numbers of cells, and therefore do not provide action potentials from single cells. More precisely, the potentials' frequencies recorded on the scalp of a normal human subject, typically vary in a range of 1–30Hz and there are only few dominant frequency bands that usually arise. They (Fig. 1) are called alpha (α, 8–13 Hz), beta (β, 13–30 Hz), delta (δ, 0.5–4 Hz) and theta (θ, 4–7 Hz). Quantitative monitoring is generally used during sleeping.

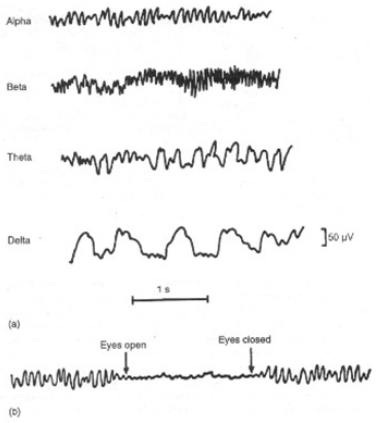

Fig. 1. (a) Different types of normal EEG waves (b), replacement of alpha rhythm by an asynchronous discharge when patient opens eye.

EEGs are useful for indirect diagnosis in order to exclude different pathologies that do not deal with what clinicians are treating. Quantitative EEGs are most used in sleeping monitoring, post-surgical activities, and resuscitation. Sleeping is regular and is featured by different stages based on electrical brain wave activities, eye movements, and muscle electrical activities. The relationship between EEG and respiratory activities is also a matter of interest since it better displays the human neurophysiology. Three main components of respiratory monitoring that influence EEG and ECG recordings during walking are: airflow, respiratory effort and arterial oxygen saturation. Exact measurement of airflow can be performed by means of a pneumotachograph [3] but for monitoring during walking process, an ergospirometer is requested [4]. Respiratory effort monitoring is necessary to classify different event. It can be measured by detecting movement of the chest and abdomen using for example piezoelectric transducers. The most sensitive method for detecting effort is monitoring of changes in esophageal pressure associated to inspiratory effort [5] in the patient under trial. Arterial oxygen saturation (SaO_2) is generally measured using pulse oximetry (finger or ear probes) [6], [7].

II. 1D-FDM Approach

The one-dimensional Filter Diagonalization Method is mostly used in signal processing as a nonlinear, parametric

Manuscript received February 27, 2013; revised May 20, 2013; accepted June 20, 2013. Date of publication June 28, 2013; date of current version July 30, 2013. The associate editor coordinating the review of this paper and approving it for publication was Dr. Harold Szu.

A. Lay-Ekuakille and P. Vergallo are with the Dipartimento d'Ingegneria dell'Innovazione, Università del Salento, Lecce 73100, Italy (e-mail: aime.lay.ekuakille@unisalento.it; patrizia.vergallo@unisalento.it).

D. Caratelli is with the IRCTR, Delft University of Technology, Delft 2628 CD, The Netherlands (e-mail: d.caratelli@tudelft.nl).

F. Conversano and S. Casciaro are with the Bioengineering Division of the Institute of Clinical Physiology, National Research Council, Lecce 73100, Italy (e-mail: conversano@ifc.cnr.it; casciaro@ifc.cnr.it).

A. Trabacca is with the Unit of Neurorehabilitation I, Developmental Neurology and Functional Rehabilitation, Scientific Institute - I.R.C.C.S. "E. Medea," Ostuni 72017, Italy (e-mail: antonio.trabacca@os.lnf.it).

Color versions of one or more of the figures in this paper are available online at http://ieeexplore.ieee.org.

Digital Object Identifier 10.1109/JSEN.2013.2271478

method for fitting time domain signals with summation of sinusoids, and especially for exponentially dumped signals. When we consider an interval of FDM, the resolution is not limited by the *Fourier Transform Uncertainty Principle*, and we can obtained high SNR with high resolution. The main scope of 1D FDM, using the Krylov base, is to define a complex one-dimensional signal in time domain $c_n = C(t_n)$, that can be defined in a set of equidistant time intervals $t_n = n\tau,\ n = 0, 1, ..., N-1$ as a sum of damped sinusoids,

$$c_n = \sum_{k=1}^{K} d_k e^{-in\tau\omega_k} = \sum_{k=1}^{K} d_k e^{-2\pi in\tau f_k - in\tau\gamma_k} \tag{1}$$

with a total of $2K$ unknowns, that is, K complex amplitudes d_s and Kcomplex frequencies $\omega_k = 2\pi f_k - i\gamma_k$ that also include damping. Even if Eq. (1) is nonlinear, its solution can be obtained from linear algebra. FDM gets in touch an autocorrelation function, in an appropriate dynamic time system described by a complex Hamiltonian operator $\hat{\Omega}$, with complex eigenvalues $\{\omega_k\}$, to signal c_n to be transformed in the form of Eq. (1):

$$c_n = \left(\Phi_0 \left| e^{-in\tau\Omega}\ \Phi_0\right.\right). \tag{2}$$

Accordingly, the problem can be simplified as a diagonalization of the Hamiltonian operator $\hat{\Omega}$ or, similarly, evolution operator $\hat{U} = \exp(-i\tau\Omega)$ as detailed in [8].

A complex inner symmetric product operation is used in Eq. (2), namely $(a|b) = (b|a)$ without a complex conjugation and Φ_0 is the initial state. Supposing we have a set of orthonormal eigenvectors $\{Y_k\}$ that diagonalize the evolution operator, that is

$$\hat{U} = \sum_k u_k\, |Y_k)(Y_k| = \sum_k \exp(-i\omega_k\tau)\, |Y_k)\ (Y_k| \tag{3}$$

and including Eq. (3) in to Eq. (2), remembering to let

$$d_k = (\Phi_0 \left| Y_k\right.)(Y_k \left| \psi_0\right.) = (Y_k \left| \Phi_0\right.)^2. \tag{4}$$

Calculated eigenvalues determine the position of spectrum lines and their widths while eigenvectors define their amplitudes and phases. Let us adopt a simple set created from Krylov vectors, generated by evolution operator: $\Phi_n = \widehat{U}^n \Phi_0 = \exp(-in\tau\hat{\Omega})\Phi_0$. According to Eq. (4), it yields to:

$$(\Phi_n \left| \hat{U}\Phi_m\right.) = (\Phi_n\, |\Phi_{m+1}\,) = c_{m+n+1} \tag{5}$$

but since the set is not orthonormal, the overlap matrix should be calculated as:

$$(\Phi_n \left| \Phi_m\right.) = (\hat{U}^n\Phi_0 \left| \widehat{U}^m \Phi_0\right.) = (\,\Phi_0|\,\hat{U}^{m+n}\Phi_0) = c_{m+n+1}. \tag{6}$$

Hence it is strictly related to values of measured signal. So the following notation could be used: $\boldsymbol{U}^0$ is a representation of $M{+}1xM{+}1$ dimensions of overlap matrix, similarly $\boldsymbol{U}^1$ is for $\hat{U}$. To signalize formulation of Eq. (1), one must solve the generalized problem of eigenvalues. In other words:

$$\mathrm{U}^1\mathrm{B}_k = u_k\mathrm{U}^0\mathrm{B}_k \tag{7}$$

in which $u_k = \exp(-in\omega_k\tau)$ gives lines of spectrum and their widths, and eigenvectors $\boldsymbol{B}_\mathrm{k}$ deliver amplitudes and phases.

A simple one-dimensional FDM algorithm can works in the following way [9]:

a) beginning from the lower frequency, in agreement with Nyquist criterion, frequency intervals $|f_{\min},\ f_{\max}|$ have been chosen for spectral analysis for sampled signal frequencies of interest $c_n = C(t_n)$, $n = 0, 1, 2, ..., N-1$. The width of the observation window allows the design of linear algebra problems to be solved in the current algorithm;

b) creating an "equispaced" grid of angular frequencies $2\pi f_{\min} < \phi_j < 2\pi f_{\max}\ ,\ j = 0, 1, ..., K_{win}$. The value of K_{win} must be chosen in the appropriate manner: in this case, as suggested by current scientific literature, $K_{win} = N(f_{\max} - f_{\min})/2\tau$ where τ is sampling time;

c) determining three complex symmetric matrices $\mathbf{U}^{(\mathrm{p})}$ of $K_{win}xK_{win}$, with $p = 0, 1, 2$. To compute the non-diagonal elements, it is necessary to use the following relationship;

$$U^{(p)}(\phi,\phi') = \frac{e^{i\phi}f_p(\phi') - e^{-i\phi'}f_p(\phi) + e^{iM\phi'}g_p(\phi) + e^{iM\phi}g_p(\phi')}{e^{-i\phi} - e^{-i\phi'}}$$
$$U^{(p)}(\phi,\phi') = \sum_{n'=0}^{M}\sum_{n=0}^{M} e^{i(\phi-\phi')}\, e^{i(n-n')\phi'}\, c_{n+n'+p} \tag{8}$$

where f_p and g_p are Fourier transforms of the first and the second parts of signal c_n respectively, with its values, in time-domain, translated in advance of p. These parts are:

$$f_p(\phi) = \sum_{n=0}^{M} e^{in\phi} c_{n+p} \tag{9}$$

$$g_p(\phi) = \sum_{n=M+1}^{2M} e^{i(n-M-1)\phi} c_{n+p} \tag{10}$$

while for computing elements out of diagonal, it is suitable to use

$$U^{(p)}(\phi,\phi') = \sum_{n=0}^{2M} (M + 1 - |m-n|)e^{in\phi} \tag{11}$$

d) solving generalized problem of eigenvalues:

$$\mathrm{U}^{(1)}\mathrm{B}_k = u_k\mathrm{U}^{(0)}\mathrm{B}_k \tag{12}$$

where eigenvalues $u_k = \exp -\omega_k\tau$ and the eigenvectors $\boldsymbol{B}_k$ are calculated by means of QZ algorithm;

e) accepting values of eigenvalues that satisfy an error criterion, so that spurious eigenvalues that can produce variations in computing parameters, can be eliminated;

f) computing complex amplitudes d_k using

$$d_k^{1/2} = \sum_{j=1}^{K_{win}} B_{jk} \sum_{n=0}^{M} c_n e^{in\phi_j} \tag{13}$$

g) using ω_k and d_k to estimate the spectrum with the following:

$$A(F) = -\sum_k Im\left\{\frac{d_k}{2\pi\, F - \omega_k}\right\}. \tag{14}$$

Physiological signals are mostly characterized by different nonstationary processes (e.g. speech, brain and heart activities, breathing, etc.) where the interested processes generate amplitude and frequency modulations. the time evolution of the fundamental frequency, in particular, challenges the stationarity assumption even inside a short analysis window. What makes FDM unique is to associate the complex signal c_n to be fitted by the form of Eq.1 with the time autocorrelation function of a fictitious dynamical system described by an effective complex symmetric Hamiltonian operator Hamiltonian operator $\hat{\Omega}$, with complex eigenvalues $\{\omega_k\}$, as indicated in Eq.(2), with complex eigenvalues. The eigenvalues, thus, determine line positions and widths, and the eigenvectors determine line amplitudes and phases. That is, one diagonalization of Eq.(12) yields all of the desired parameters. This is again in contrast to linear predictor (LP), in which a singular value decomposition (SVD) or similar procedure is used to find the LP coefficients, a polynomial rooting or equivalent procedure is then used to determine line frequencies and widths, and then another least squares problem, using these roots as input, must be solved to determine amplitudes and phases in nonstationary conditions. Hence, FDM is a very powerful tool for nonstationary conditions.

III. Proposed 2D-FDM Algorithm for Multispectrum and Experimentations

To the best of our knowledge, its multidimensional versions hardly have competing analogues. Although, for some one-dimensional (1D) problems, especially involving very long and noiseless signals, FDM is extremely efficient, its actual strength is revealed outside of the 1D applications according to the re-written Eq. (15) that is the Eq.(1).

$$c_a(t) = \sum_{k=1}^{K} d_k e^{-j w_k}. \tag{15}$$

The basic reason is that FDM processes the whole multi-dimensional data set simultaneously by fitting it to a certain multi-dimensional parametric form, unlike the FT spectral analysis which is intrinsically 1D. For instance, 2D FDM [10] can be written as

$$c(t_1, t_2) = \sum_{k=1}^{K} d_k e^{-j t_1 w_{1,k}} e^{-j t_2 w_{2,k}} \tag{16}$$

with $\omega_{1,k}$, $\omega_{2,k}$ and d_k now characterizing the 2D spectral features. By solving Eq. (16) one can, in principle, obtain high spectral resolution even if the signal is not available at both long t_1 and t_2, as would be required by the Fourier uncertainty principle. It is the total size of the 2D data set, which implies the total number of algebraic equations with the unknowns $\{d_k, \omega_{1,k}, \omega_{2,k}\}$ and which is relevant. Experimentally, it may be easy to satisfy the condition when the total number, $N1 > N2$; of the 2D signal points, i.e. the number of equations, dominates the total number of unknowns $(3K)$. In a 1D signal processing scheme the length of the signal in each dimension has to dominate the number of unknowns, i.e. $N1 > 2K$ and $N2 > 2K$. A method implemented in the frame of 2D FDM, called "simultaneous diagonalization",

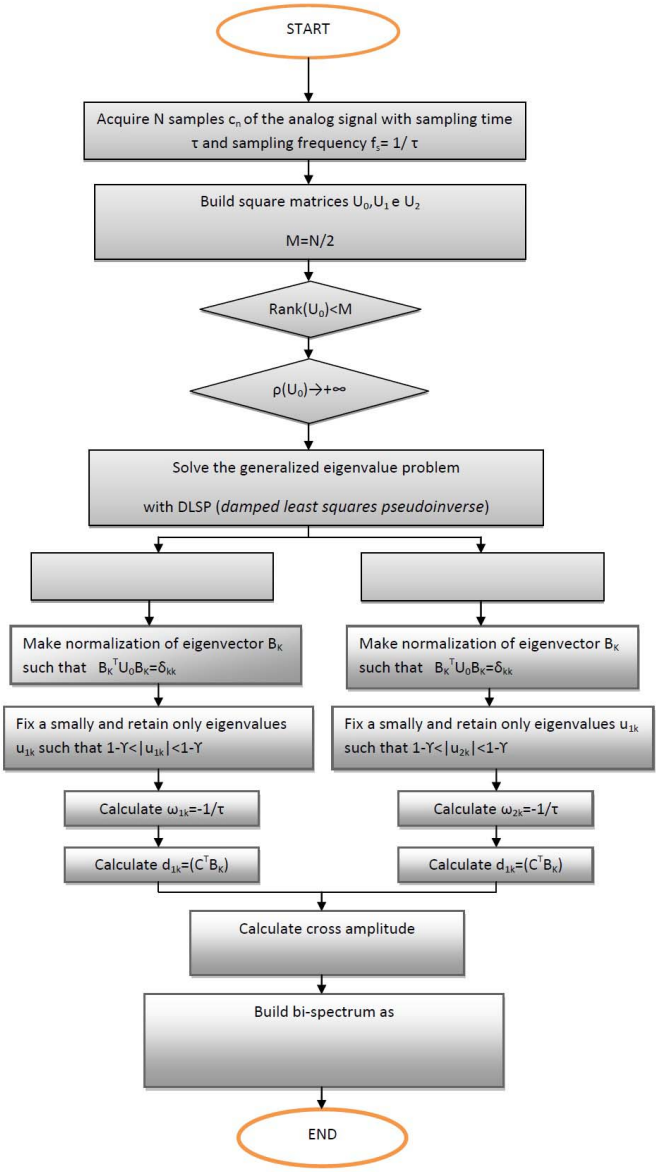

Fig. 2. 2D-FDM algorithm flowchart.

was suggested to overcome this degeneracy problem. It was argued later that the degeneracy itself does not actually create any numerical problem, if the SNR is sufficiently high, an artifact free spectrum can be constructed by using the resolvent operator (or Green's function) approach. Rather than Eq.(16), this approach implies a much more pessimistic, direct-product, parametric form to represent the 2D time domain data

$$c(t_1, t_2) = \sum_{k_1=1}^{K_1} \sum_{k_2=1}^{K_2} d_{k_1 k_2} e^{-j t_1 w_{1,k_1}} e^{-j t_2 w_{2,k_2}}. \tag{17}$$

Although this equation is not solved explicitly for the unknowns d_{k1k2}, ω_{k1} and ω_{k2}. The reason is that for a general 2D data array $c(t_1, t_2)$. Eq. (16) is ill defined or in other words, the solution is very sensitive to both the parameters of the fit (such as K) and small perturbations of $c(t_1, t_2)$. This sensitivity causes instability of the result for a noisy input, appearing in the FDM spectra in a wild nonlinear fashion as spurious spikes or errors in the amplitudes and phases of the genuine features.

The complete 2D algorithm, applied for this circumstances, is depicted in Fig. 2.

The majority of methods using fast multidimensional techniques (e.g., Laplace transform, non-negative independent component analysis, linear predictors, Prony method, MUSIC, ESPRIT, etc..) require that the pulse sequence be altered in such a way as to preclude standard processing techniques. This can make it difficult to directly evaluate the performance of the method as compared to conventional methods such as the Fourier transform (FT) or mirror-image linear prediction (MI-LP). FDM is a powerful method for the generation of high-resolution spectral estimates from data sets having far fewer increments in the indirect dimensions.

Hence, for multidimensional cases, while the number of points in each indirect dimension may be small, their product is very large. This improves the resolving capabilities of the FDM relative to orthogonal processing methods. To avoid time consuming operations, for facing very large products, we have implemented QZ algorithm to improve the output of Eq.(12). In addition to FDM approach, high order spectra (HOS) are also used for processing signals in a comparative way. HOS analysis [11] offers diverse advantages, among them it is suitable to find the extra information provided by the analysis to better estimate parameters and sheds light on nonlinearities in the source of the signal. Different indicators can be calculated inside the non – redundant region because one of the properties of the bispectrum is that to show symmetry of regions. In this work FDM method is used to obtained the bispectrum, allowing an improvement in the resolution of the features of the EEG signals. The objective is to extract important information to help during diagnosis of the patients suffering from epilepsy or other neuropathologies. In this analysis an important parameter obtained through ECG test has been used: HRV (Heart Rate Variability). HRV is an useful element for analyzing the heart rate variability. It is important because different information can be deduced to evaluate the risk of cardiac arrhythmias, or heart attack, as well as of the balance between the sympathetic and parasympathetic nervous system. So it is the natural variability of heart rate in response to factors such as the rate of breathing, emotional, and heart rate of an heart healthy responds quickly to all these factors, changing depending on the situation.

Once the algorithm for two-dimensional application has been defined, now we can describe the experimental setup for acquiring data thanks to a joint and simultaneous acquisition of EEGs, ECGs and ergospirometric data. For the purposes of this research two children (age around 10 years) have been involved and they walked on a corridor of around 30 meters. The main scope is to evaluate neurophysiology due to eventual difficulty in walking and standing in equilibrium, and verifying the compatibility between the physical effort parameters, namely heart rate variability (HR), cardiac fitness index (CFI), oxygen consumption and VO_2. This latter measures concentrations of in the expired air by human body during a maximum trial. The above parameters have a great impact on the neurological system and vice versa. Fig. 3 illustrates two particular moments. The first one is the setup operations for the first child (up) and the second is the trial for the second child (bottom). The children are under trial for suspected case of epilepsy. Further descriptions of the trials are described in [12].

Fig. 3. Experimental acquisition setup (up) and working (bottom).

IV. Comparative Acquisitions and Processing With ECG and Ergospirometer

The influence of walking and striding on neurophysiology is well-known since many factors are involved, namely, breathe, fatigue, stress, oxygen circulation in the organism, oxygen flow in the brain, etc. However, direct and simultaneous joint measurements of features from ECG, ECG and ergospirometer are not often performed since it is very difficult to do in children. Two patients are considered. Following their heart rate variability is shown. Two portions of the signal are taken into account for the first patient and two for the second equal to the amount of recorded data. One of the regions considered is where heart rate is more variable and by the analysis of the EEG we want to know the cause. If for example the spikes are present in the EEG recorded, it can be reflected in HRV and vice versa. In general, abnormalities in the EEG are due to the presence of slow wave with high amplitude. Heart Rate should

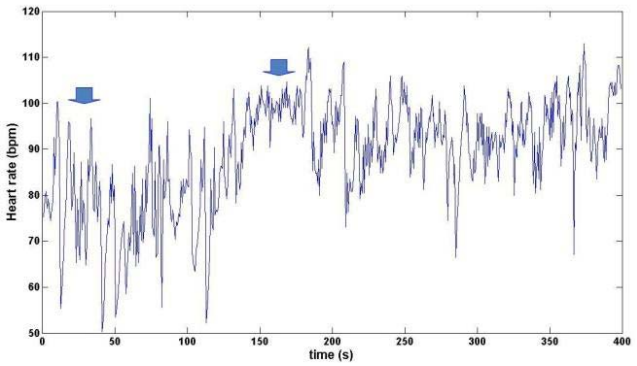

Fig. 4. HR for the first patient.

respond to this issue. If it is not, the study of the bispectrum could be of great help.

The two patients are children and the second one is suspected of suffering from epilepsy. Two individuals are sufficient since they are from the group of ten included in previous work as indicated in [12] which scope is different from that included in the current paper.

V. Results and Discussion

The tests have a duration of about 6/7 minutes to allow an assessment of the changes in the parameters of interest during the trial. Usually, in clinical analysis the characteristic frequencies of the recorded signals are analyzed considering the samples relating to a period, that is those acquired in a second. The sampling frequency is about 256 Hz, so in a second the available samples are 256. So, one can perform the analysis on short periods of recorded traces and evaluate the frequency content. We have applied the methods of analysis of the different periods, from 2 to 5, considering the most significant from a clinical viewpoint related to HRV too.

Once the signals have been acquired, they have been processed according to the above FDM algorithms, that are 1D and 2D. A further processing using HOS has been also performed. We start with the calculation of HR even it has been acquired thanks to ergospirometry; but it can be extracted from the ECG signal. For each children the following parameters have been computed and processed: HR, from EEG FDM-based contour, a magnitude bispectrum using FDM and the same with HOS, and a bicoherence map. In Fig. 4 the heart rate of the first patient under observation is shown.

Heart rate mean value of this patient is 88 bpm. The blue arrows indicate two portions of the heart rate variability. In the first part there is a strong variation of the heart rate, while following the signal settles down around its average mean. Relatively to the first portion of HR, the EEG signal of Fig. 5 is considered. We report the EEG relative to one of the 19 electrodes placed on the scalp.

In Fig. 6 the absorption spectrum is reported. There is a peak at 50 Hz frequency (red arrow) because notch filter, used by the clinicians during the experimental recording, was off.

A significant peak is detected in the lower frequency of EEG (see green arrow). So, FDM bispectrum allows to point out slow waves with a great amplitude because these frequencies

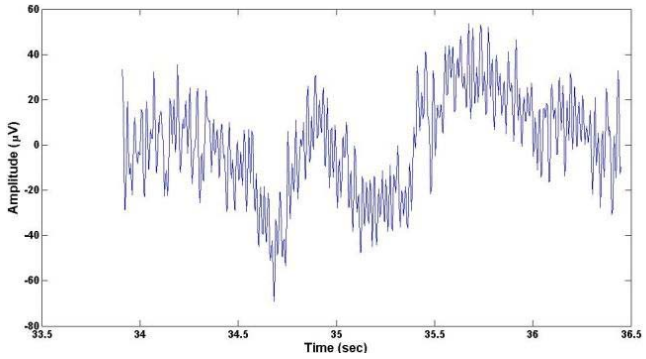

Fig. 5. EEG first patient, first interval.

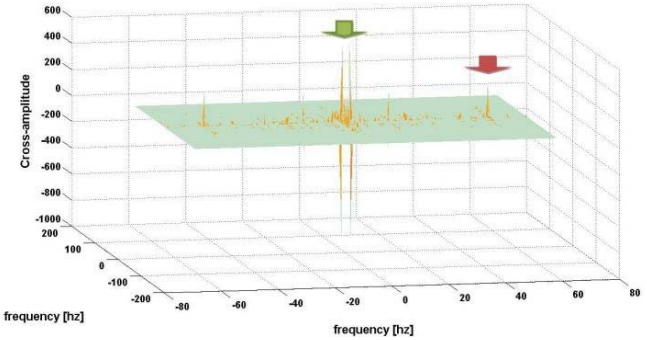

Fig. 6. Absorption Spectra by FDM for the first patient.

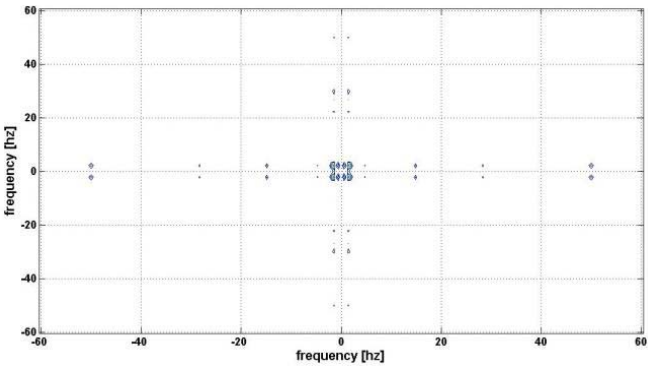

Fig. 7. Contour of FDM bispectrum.

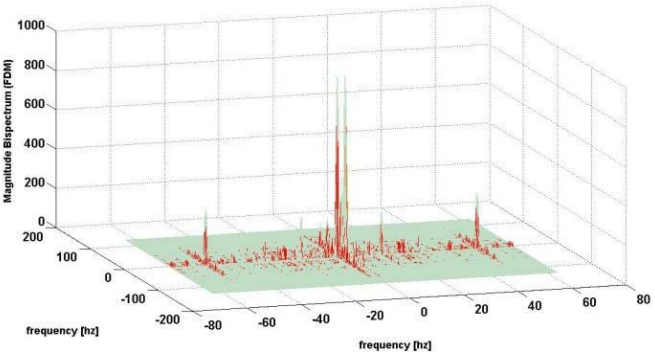

Fig. 8. Magnitude bispectrum FDM.

are dominant in the bispectrum. This property of the FDM is evident in Fig. 7, where the contour of FDM bispectrum shows the important frequency included in the considered EEG signal.

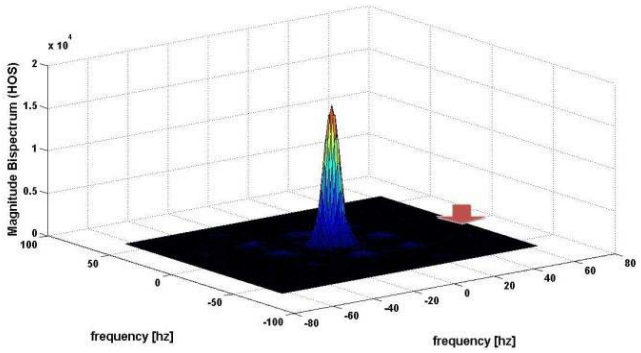

Fig. 9. Magnitude bispectrum with HOS.

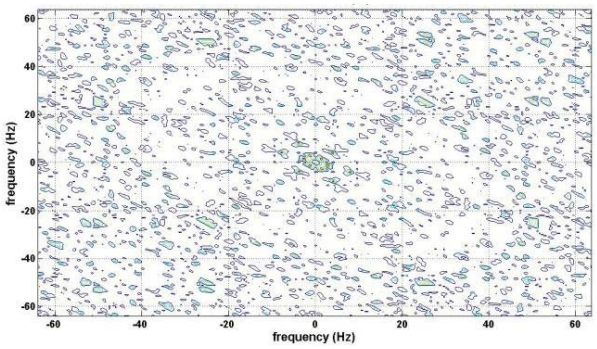

Fig. 10. Bicoherence of the first patient.

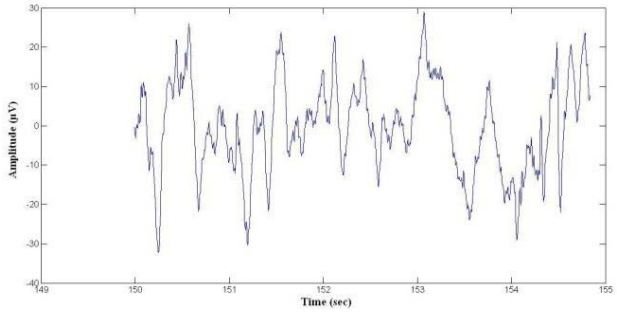

Fig. 11. Second part of EEG first patient.

In Fig. 8 the magnitude bispectrum is shown even if it delivers the same information of the absorption spectrum of figure 6 but with a clear vision of the different peaks encompassed in the EEG.

As comparison, techniques using HOS are applied to the same signal. In Fig. 9 the bispectrum obtained by Fourier transform of the third-order statistics is reported. In this case, as in the previous one, the red arrow highlights the 50 Hz frequency, but the information to lower frequency is lost while in the FDM approach it is preserved. That is one of the reasons of the strength and the power of FDM. So, in this case, the calculation of the magnitude bicoherence index is more important because the red points (Fig. 10) indicate peaks to low frequency, but the contour of FDM bispectrum is more efficient in terms of resolution as it can be seen from Fig. 7. Spectral magnitude mean of FDM and HOS methods is calculated as the mean value of the magnitude of the peaks

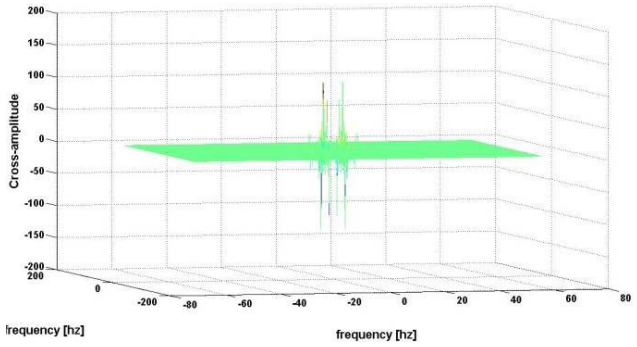

Fig. 12. Absorption spectra of second part of first patient EEG.

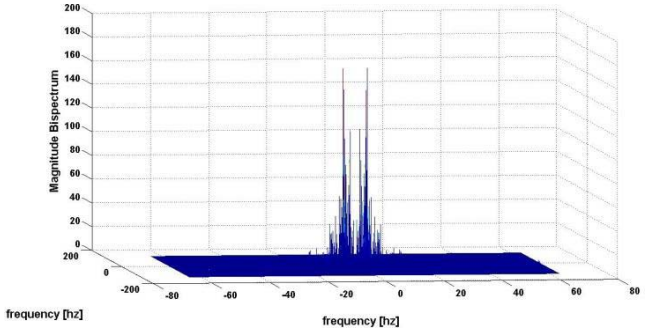

Fig. 13. FDM magnitude spectrum for second part of first patient.

in the bispectrum. It is a parameter necessary for evaluating the performance of both methods in short terms.

So we have obtained the following values:

- spectral magnitude mean based on FDM: 275.13;
- spectral magnitude mean based on HOS: 149.32.

In order to achieve the goal of the paper, the EEG signal in Fig. 11 is the one corresponding to the second part of HRV of the first patient.

Analogously, all features are reported, we mean: absorption (Fig. 12) and magnitude spectra (Fig. 13), FDM bispectrum contour (Fig. 14), HOS bispectrum (Fig. 15) and bicoherence (Fig. 16). The following values are also calculated:

- Spectral magnitude mean for FDM: 5.6;
- Spectral magnitude mean for HOS: 1.36×10^4.

In this second case FDM highlights a clear predominant activity at 4 Hz compared to the HOS. So, for the first patient FDM exhibits a high resolution with respect to HOS. Peaks are more narrow and this fact allows to display many features.

That is the reason, in the second case of the first patient, we would have expected a spectral magnitude mean of HOS less than that we have found for FDM because the brain activity is concentrated only around low frequencies and therefore more contained; but the low resolution, due to the choice of interval, does not permit to distinguish signal characteristics at low frequencies in HOS method.

As for the first patient analysis, we start with the second one, performing the same analysis. The HR trend is reported, and two intervals are under analysis. Its mean value is 99 bpm. An EEG signal relative to first part is reported in Fig. 18 using signal of Fig. 17.

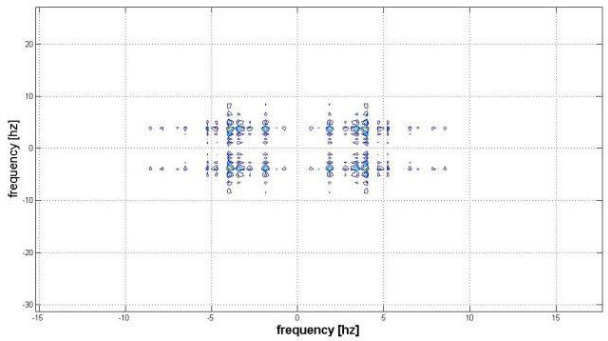

Fig. 14. FDM contour bispectrum.

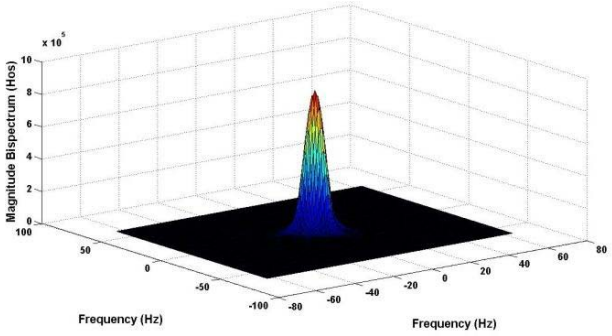

Fig. 15. Magnitude bispectrum with HOS.

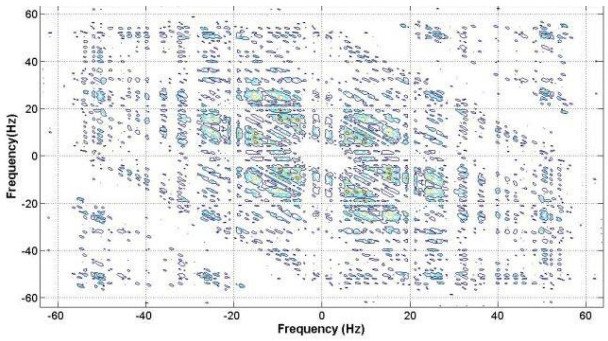

Fig. 16. Bicoherence.

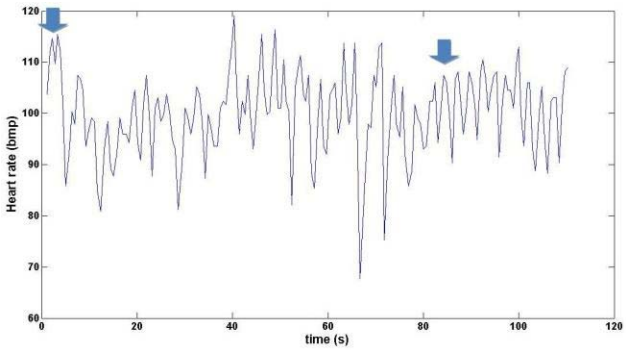

Fig. 17. HR for the second patient.

In the absorption spectrum (Fig. 19) it is possible to see peaks around 1–1.5 frequencies. So we see these peaks as spikes which cause an abnormal behavior in brain activity. This feature, in the trend of EEG signal, can be observed in Fig. 20 and Fig. 21. HOS bispectrum is shown in figure 22, while in figure 23 the bicoherence is reported.

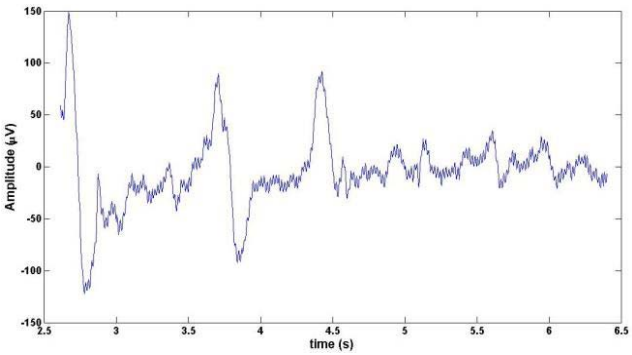

Fig. 18. First part of EEG of the second patient.

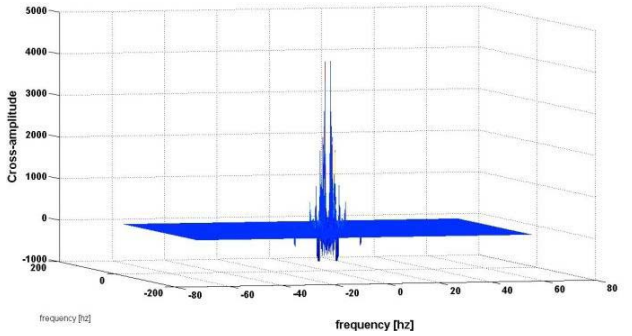

Fig. 19. FDM absorption spectrum for the second patient.

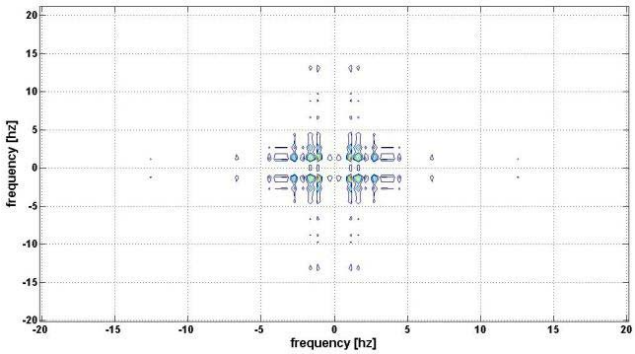

Fig. 20. FDM contour spectrum.

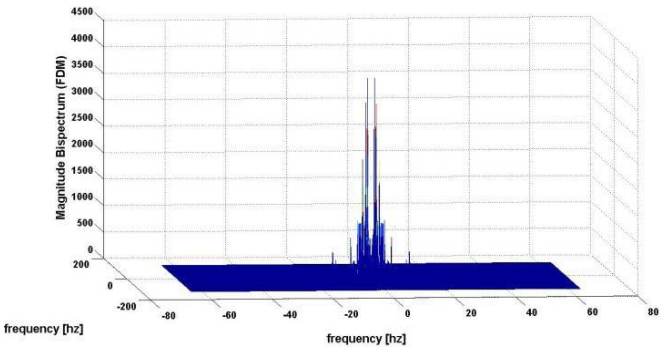

Fig. 21. FDM magnitude spectrum for the first part of second patient.

The following values are also calculated:
- spectral magnitude mean for FDM: 1007.2;
- spectral magnitude mean for HOS: 4.52×10^4.

These mean values are great with respect to the previous ones for the presence of slow and large waves. In Fig. 24 the

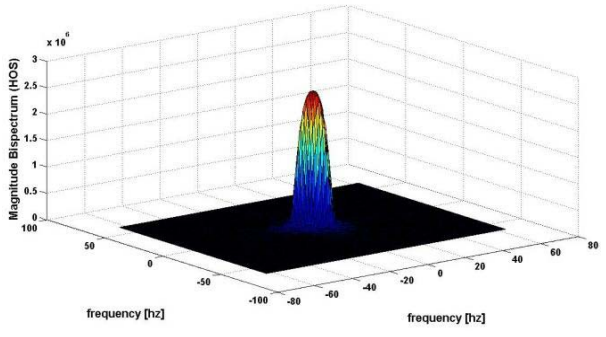

Fig. 22. Magnitude bispectrum with HOS.

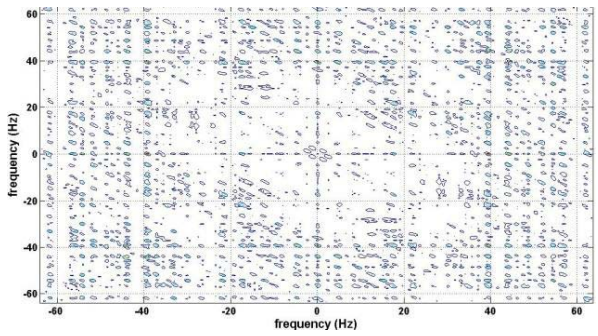

Fig. 23. Bicoherence.

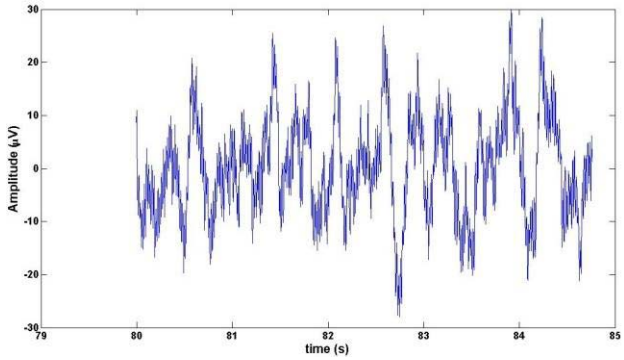

Fig. 24. Second case of the second patient.

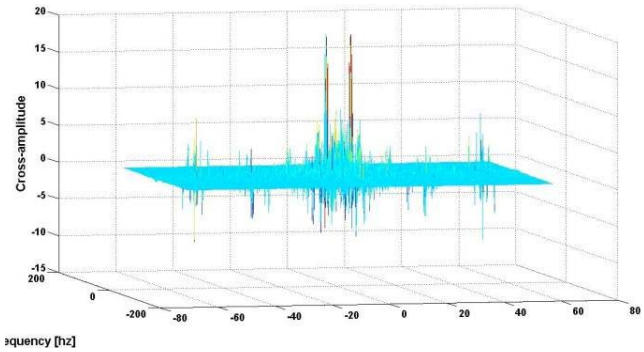

Fig. 25. Absorption spectra-second case of second patient.

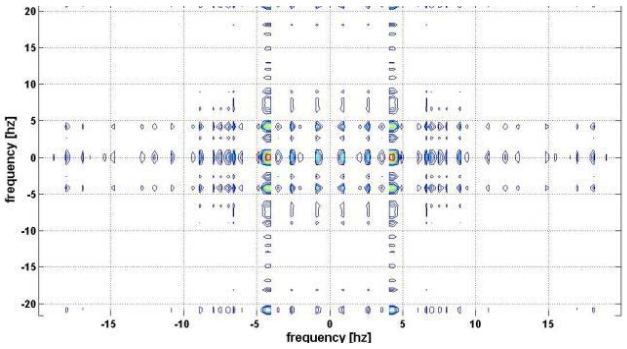

Fig. 26. FDM contour.

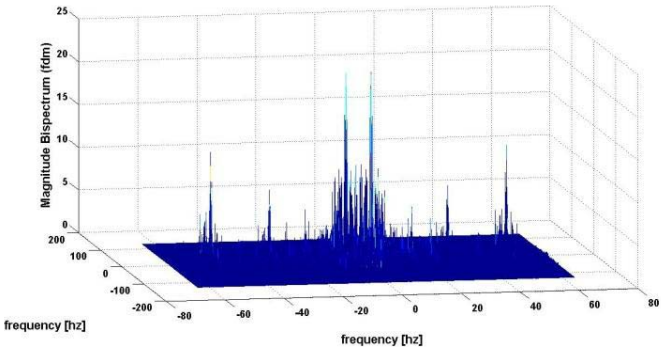

Fig. 27. Magnitude bispectrum.

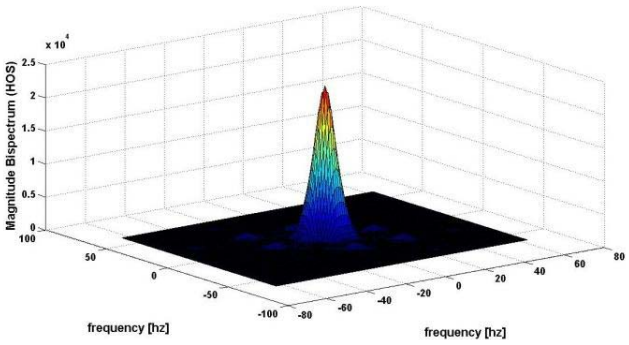

Fig. 28. Magnitude bispectrum with HOS.

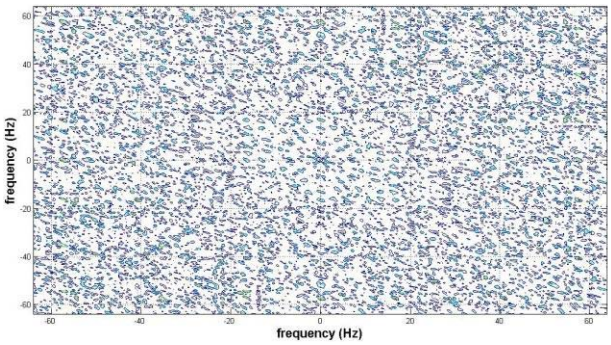

Fig. 29. Bicoherence.

second part of the EEG signal for the second patient is shown, and its bispectrum (Fig. 25).

The calculated mean values are:

- spectral magnitude mean for FDM: 5.26;
- spectral magnitude mean for HOS: 373.83.

These values would indicate, for the considered range, a normal brain activity and which is stabilized around its mean value (99 bpm) as shown in Fig. 17. Analogously, using the second of the signal, FDM contour (Fig. 26), magnitude bispectrum (Fig. 27), Magnitude bispectrum with HOS (Fig. 28),

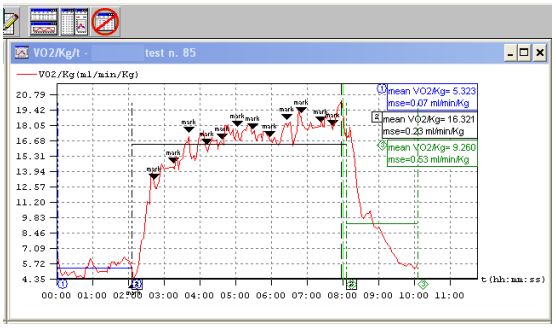

Fig. 30. Patient 1 oxygen uptake measured using ergospirometer.

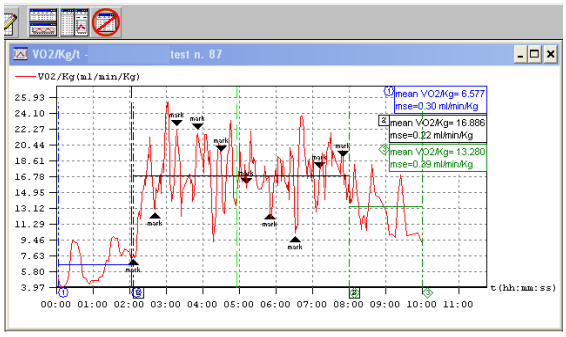

Fig. 31. Patient 2 oxygen uptake measured using ergospirometer.

and bicoherence (Fig. 29) are computed. Even in this case, HOS does not preserve low frequencies, so there is a loss of information at certain frequencies.

VI. Conclusion

Before the final gloss of this paper, we would like to recall the importance of joint measurements for complete processing of signals in a multidimensional approach. We have discussed in the previous section about the interesting characteristics displayed by FDM with respect to HOS in the effort to enhance neurophysiological aspects encompassed in the signals under process prior specific measurements, that means, prior EEG, ECG and ergospirometry. Fig. 30 and Fig. 31 illustrate the oxygen uptake per child that is correlated to the HR, absorption spectra, FDM contour, and peaks related to bicoherence matrix. For the first child the regularity of oxygen uptake is confirmed by the narrowness of magnitude spectrum, and of the absorption spectra that are related to the concentration of the peaks of VO_2 trend before the end of the physical effort as depicted in Fig. 30. That is also related, but immediately, to the trend of EEG signals in both foreseen ranges. Conversely, VO_2 trend (Fig. 31) indicates that the second child produces a great effort in walking, both EEG signals for the envisaged intervals show what happens; that is also correlated to the distribution of peaks on magnitude spectrum, and absorption spectra figures. This distribution allows to understand the oxygen uptake necessary for brain functioning. However HOS does not clearly point out the issue related to neurophysiological aspects. Further confirmation is given by Fig. 25 with manifold peaks. Hence, the research shows that it is possible to use only two instruments instead of three to better understand the neurophysiology of individuals suspected of suffering from neuropathologies as for example epilepsy.

The proposed study is also suitable for studying premature risks of cardiac arrest in children related to EEG activities. Cardiac arrest has a devastating effect on the neurophysiology, in spite of numerous clinical trials, neuroprotective agents have failed to improve outcome statistics after cardiac arrest [13], [14]. It is also an interesting approach for studying absence seizure generation in a spatial-temporal issues since FDM acts as a spatial filtering [15].

Acknowledgment

Authors are in debt with F. Angelillo and M. De Rinaldis who are with the IRCCS “E. Medea”, Associazione “La Nostra Famiglia” for their great help during this work.

References

[1] A. Lay-Ekuakille, G. Vendramin, and A. Trotta, “Beamforming-aided processing of EEG signals for analyzing epileptic seizures,” *Int. J. Adv. Media Commun.*, vol. 3, pp. 110–125, Jun. 2009.
[2] N. Mammone, G. Inuso, F. La Foresta, M. Versaci, and F. C. Morabito, “Clustering of entropy topography in epileptic electroencephalography,” *Neural Comput. Appl.*, vol. 20, no. 6, pp. 825–833, 2011.
[3] A. Lay-Ekuakille, G. Vendramin, and A. Trotta, “Spirometric measurement post-processing: Expiration data recovery,” *IEEE Sensors J.*, vol. 10, no. 1, pp. 25–33, Jan. 2010.
[4] P. Vergallo, A. Lay-Ekuakille, A. Trotta, A. Trabacca, M. De Rinaldis, F. Angelillo, and L. Petrara, “Improving ergospirometric sensing capability through optimized denoising,” in *Proc. 4th ICST*, Jun. 2010, pp. 1–3.
[5] R. B. Berry, “Nasal and esophageal pressure monitoring,” in *Sleep Medicine*, T. L. Lee-Chiong, M. J. Sateia, and M. A. Caraskadon, Eds. Philadelphia, PA, USA: Hanley and Belfus, 2002, pp. 661–671.
[6] L. Gbaoui and E. Kaniusas, “Decomposition of photoplethysmographical arterial pulse waves by independent component analysis,” in *Proc. Adv. Biomed. Sens., Meas., Instrum. Syst., Lecture Notes Electr. Eng.*, vol. 55. 2010, pp. 166–185.
[7] A. Lymberis, “Advanced wearable sensors and systems enabling personal applications,” in *Proc. Wearable Auto. Biomed. Devices Syst. Smart Environ., Issues Characterization, Lecture Notes Electr. Eng.*, vol. 75. 2010, pp. 237–257.
[8] V. A. Mandelshtam and H. S. Taylor, “Harmonic inversion of time signals and its application,” *J. Chem. Phys.*, vol. 107, no. 17, pp. 6756–6769, 1997.
[9] A. Lay-Ekuakille, G. Vendramin, and A. Trotta, “Robust spectral leak detection of complex pipelines using filter diagonalization method,” *IEEE Sensors J.*, vol. 9, no. 11, pp. 1605–1614, Aug. 2010.
[10] J. Chen, V. A. Mandelshtam, and A. J. Shaka, “Regularization of the two dimensional filter diagonalization method: FDM2K,” *J. Magn. Resonance*, vol. 146, no. 2, pp. 363–368, 2000.
[11] C. L. Nikias and J. M. Mendel, “Signal processing with high-order spectra,” *IEEE Signal Process. Mag.*, vol. 10, no. 3, pp. 10–37, Jul. 1993.
[12] A. Lay-Ekuakille. P. Vergallo, A. Trabacca, M. De Rinaldis, F. Angelillo, F. Conversano, and S. Casciaro, “Low-frequency detection in ECG signals and joint EEG-ergospirometric measurements for precautionary diagnosis,” *Measurement*, vol. 46, no. 1, pp. 97–107, 2013.
[13] Brain Resuscitation Clinical trial II Study group, “A randomized clinical trial of calcium entry blocker administration to comatose survivors of cardiac arrest: Designa, methods, and patient characteristics, *Control Clinical Trials*, vol. 12, no. 4, pp. 525–545, 1991.
[14] W. T. Longstreth, Jr., C. E. Fahrenbruch, M. Olsufka, T. R. Walsh, M. K. Copass, and L. A. Cobb, “Randomized clinical trial of magnesium, diazepam, or both after out-of-hospital cardiac arrest,” *Neurology*, vol. 59, no. 4, pp. 506–514, 2002.
[15] N. Mammone, D. Labate, A. Lay-Ekuakille, and F.C. Morabito, “Analysis of absence seizure generation using EEG spatial-temporal regularity measures,” *Int. J. Neural Syst.*, vol. 22, no. 6, pp. 1250024-1–1250024-40, 2012.
[16] A. Lay-Ekuakille, P. Vergallo, G. Griffo, F. Conversano, S. Casciaro, S. Urooj, V. Bhateja, and A. Trabacca, “Mutidimensional analysis of EEG features using advanced spectral estimates for diagnosis accuracy,” in *Proc. IEEE Med. Meas. Appl.*, May 2013, pp. 1–3.

Aimé Lay-Ekuakille is with the University of Salento, Lecce, Italy. He received the M.D. degree in electronic engineering, the M.D. degree in clinical engineering, the Ph.D. degree in electronic engineering, and the Post Degree in environmental impact assessment. He was a Director of Instrumentation and Measurement Laboratory, University of Salento. He is currently a Scientific Advisor with the Italian National Committee for Integrated Pollution Prevention and Control, and Health Issues and a Senior Advisor with the Italian Ministry of Environment. Since January 2010, he has been serving as an Untenured Associate Professor of measurements and instrumentation with MMC, Nairobi, Kenya, and a Guest Professor of sensor signal processing with Chemnitz Technical University, Chemnitz, Germany. He is on the boards of different international journals, including an Associate Editor of the IEEE SENSORS JOURNAL. His main research interests include environmental, industrial and biomedical instrumentation and measurements even using nanotechnology devices, and renewable energy. He has authored or co-authored more than 150 papers on international journals and proceedings. He has co-edited three international books and authored or co-authored two international books (in progress).

Patrizia Vergallo received the master's degree in automation engineering from the University of Salento, Lecce, Italy, in 2009. She is currently with the Measurements and Instrumentation Scientific Group, University of Salento, with a grant as a Ph.D. Student. Her main research interests include biomedical and environmental measurements and instrumentation. Her area of expertise is modeling, processing and design requirements of sensing systems and measurement information from sensors.

Diego Caratelli was born in Latina, Italy, on May 2, 1975. He received the Laurea (*summa cum laude*) and Ph.D. degrees in electronic engineering, and the M.Sc. degree (*summa cum laude*) in applied mathematics from the Sapienza University of Rome, Rome, Italy in 2000, 2004, and 2013, respectively.

From 2007 to 2013, he was a Senior Researcher with the International Research Centre for Telecommunications and Radar, Delft University of Technology, Delft, The Netherlands. Since 2013, he has been with The Antenna Company Nederland B. V., Eindhoven, The Netherlands, as a Director of research and development. His main research interests include the full-wave analysis and design of passive devices and antennas for satellite, wireless and radar applications, the development of analytically-based numerical techniques devoted to the modeling of wave propagation, and diffraction processes. He has published more than 100 publications in international journals, book chapters, and conference proceedings.

Francesco Conversano is a Research Scientist with the National Research Council, Institute of Clinical Physiology, Lecce, Italy. His main research interests include the development of new methods for non-invasive tissue characterization, innovative strategies for nanoparticle-aided non-ionizing molecular imaging, and implementation of novel algorithms for biomedical signal processing.

Sergio Casciaro received the Laurea degree in nuclear engineering from the Turin Polytechnic Engineering School, Politecnico di Torino, Torino, Italy, and the Ph.D. degree in bioengineering from the University of Pisa, Pisa, Italy. Since 2002, he has been a Research Scientist with the National Council of Research, Institute of Clinical Physiology, Lecce, Italy, as the Head of the Biomedical Engineering Science and Technology Division and the Director of the Nanoimaging Ultrasound LAB for cellular and molecular imaging through innovative nanosystems for diagnosis and therapy.

Antonio Trabacca received the Degree in medicine and surgery from the University of Bari, Bari, Italy, in 1990, the Post-Graduate degree in neurology from the University of Bari, a Postdoctoral training in electromyography and neurophysiology with the University of Ferrara, Ferrara, Italy, and the M.S. degree in health management from the SDA–Bocconi School of Management, Milano, Italy, in 2002. He is currently the Head Physician of the Unit of Neurorehabilitation I with the Scientific Institute I.R.C.C.S. "Eugenio Medea" – Association "La Nostra Famiglia," Ostuni – Brindisi-Research Center. He is the Health Director of the Institute I.R.C.C.S. "Eugenio Medea" – Ostuni – Brindisi. He is the author of several papers of neurologic matter. Currently, he is actively working to further research in paediatric epileptology, electroencephalography, and clinical neurophysiology and in advanced MRI techniques to determine the structural changes in brain structure related to normal brain development.